Computational Materials Science 85 (2014) 310–315

Contents lists available at ScienceDirect

Computational Materials Science

journal homepage: www.elsevier.com/locate/commatsci

Detailed DFT studies of the band profiles and optical properties of antiperovskites $SbNCa_3$ and $BiNCa_3$

M. Bilal [a], Iftikhar Ahmad [a,*], H.A. Rahnamaye Aliabad [b], S. Jalali Asadabadi [c]

[a] Center for Materials Modeling and Simulations, University of Malakand, Chakdara, Pakistan
[b] Department of Physics, Hakim Sabzevari University, Sabzevar, Iran
[c] Department of Physics, Faculty of Science, University of Isfahan, HezarGerib Avenue, Isfahan 817446-73441, Iran

ARTICLE INFO

Article history:
Received 6 October 2013
Received in revised form 18 November 2013
Accepted 16 December 2013

Keywords:
Antiperovskites
Electronic band structure
Density of states
DFT
Optical properties

ABSTRACT

Structural, electronic and optical properties of antiperovskite compounds, $SbNCa_3$ and $BiNCa_3$, are studied by using the full-potential linearized augmented plane waves (FP-LAPW) method under the framework of density functional theory (DFT). The exchange–correlation potential is treated by local density approximation (LDA), generalized gradient approximation (GGA-PBEsol) and GGA developed by Engel and Vosko (EV-GGA). Furthermore, the modified Becke–Johnson (mBJ) potential is also applied to attain reliable results for the band gaps of these compounds. The calculated lattice constants are found consistent with the experimentally measured values and other theoretical results. The band profiles show that both of these materials are direct band gap semiconductors of about 1.1 eV gap. The direct band gap nature reveals that they may be effective in optical devices and therefore the optical properties of these compounds like the real and imaginary parts of dielectric function, refractive index and absorption coefficient are also calculated and discussed.

1. Introduction

Ternary carbides and nitrides having cubic antiperovskite structure are emerged as promising compounds for different technological applications. These materials have gained importance as they display variety of physical properties such as giant magnetoresistance [1], nearly zero temperature coefficients of resistivity [2] and wide range of band gaps, from super conductor to insulator [3,4]. The general formula for these compounds is AXB_3, where A is group III–V element, X is carbon or nitrogen and B is s–d metal [5,6]. These materials crystallize in cubic structure with space group Pm3m (#221). The A atoms are positioned at (0, 0, 0) coordinates, X atoms at (0.5, 0.5, 0.5) and B atoms at (0, 0.5, 0.5) of the unit cell.

Chern et al. [7] reported the synthesis of $ANCa_3$ (A = P, As, Sb and Bi) materials by mixing and pressing Ca_3N_2 powders and group V elements into a pellet and subsequently heating the pellets at 1000 °C in the flowing dry N_2 gas. They observed semiconducting nature for $SbNCa_3$ and $BiNCa_3$ compounds. In the same year, the electronic structure and bonding properties of $BiNCa_3$ and $PbNCa_3$ materials were studied by Papaconstantopoulos and Pickett [8] using the augmented plane-wave method. They are of the opinion that the bandgap of these compounds is very narrow, about 0.07 eV for $BiNCa_3$. A few years later the structural properties of $AsNCa_3$, $PNCa_3$ and $BiNCa_3$ were investigated by Vansant et al. [9] using local density approximation (LDA) and are also of the opinion that $BiNCa_3$ is a narrow band gap semiconductor. In a relatively recent studies, Haddadi et al. [10] investigated the pressure dependent elastic properties of $ANCa_3$ (A = P, As, Sb and Bi) using the plane wave pseudo-potential method, while Moakafi et al. [11] explored the elastic, electronic and optical properties of $SbNCa_3$ and $BiNCa_3$ using a full relativistic version of the full-potential linearized augmented plane-wave plus local orbitals method based on the density functional theory.

The results reported in Ref. [11] contradict the claim of the authors that "$SbNCa_3$ and $BiNCa_3$ are semiconductors in nature". As the figures of the band profiles presented in the article clearly show that for both materials the top of valance band crosses the Fermi level and enters into the conduction band and hence these materials are not semiconducting, which is also in disagreement with the experimental results [7]. In the present article, this anomaly is addressed with great care using different theoretical techniques, based on the full potential linearized augmented plane waves (FP-LAPW) method, like local density approximation (LDA), generalized gradient approximation (GGA), Engel–Vosko GGA (EV-GGA) and modified Becke–Johnson (mBJ) potential. It is expected that the present work will not only rectify the errors in the existing theoretical work, but will also provide a realistic picture of the compounds which will be helpful in understanding

* Corresponding author. Tel.: +92 332 906 7866.
E-mail address: ahma5532@gmail.com (I. Ahmad).

0927-0256/$ - see front matter © 2013 Elsevier B.V. All rights reserved.
http://dx.doi.org/10.1016/j.commatsci.2013.12.035

various physical properties of these compounds and will also identify their potential applications in optical and optoelectronic devices.

2. Computational details

In this paper FP-LAPW method within the framework of DFT [12,13] as implemented in the WIEN2k package [14] is used to calculate the structural, electronic and optical properties of $SbNCa_3$ and $BiNCa_3$. In addition to LDA, GGA and EV-GGA, we have also used the mBJ exchange potential [15,16] assembly with GGA to handle the exchange–correlation for achieving better band gaps.

The separation energy, in the present calculations, between the core and valence states is −6.0 Ry. The wave functions inside the atomic spheres for both materials, in the full potential scheme, are expanded in terms of spherical harmonics up to $l_{max} = 10$. To ensure the total energy convergence R_{MT}'s are fixed as 2.5, 2.23 and 2.34 Bohr for $SbNCa_3$ and 2.5, 2.25 and 2.36 Bohr for $BiNCa_3$. For both compounds the plane wave cutoff values, $R_{MT}K_{max}$'s, for the wave functions in the interstitial region are optimized. The optimization curves are shown in Fig. 1. The results show that the optimized value for the dimensionless $(R_{MT}K_{Max.})_{Opt.}$ parameter is 8 for which the total energy is reliably converged for both of the compounds, see Fig. 1. Therefore, in this work the $R_{MT}K_{max}$ parameter is adjusted to $(R_{MT}K_{Max.})_{Opt.} = 8$. The plane wave cutoff value for the charge density and potential is selected to be $G_{Max.} = 14$ $(Ry)^{1/2}$. The electronic and optical properties are performed using 2300 k-points in the irreducible Brillouin zone.

3. Results and discussion

3.1. Structural properties

To obtain the ground-state properties such as the equilibrium lattice parameter a_o and bulk modulus B_o for $SbNCa_3$ and $BiNCa_3$ materials, the total energy–volume curves are calculated and fitted to the Birch–Murnaghan's equation of state [17]. We obtained lattice constants and bulk moduli for these materials using LDA, PBE-GGA, PBEsol-GGA, WC and three versions of EV-GGA, see Fig. 2. There are three potential options for applying EV-GGA in these calculations which are called EV1, EV2, and EV3. In the first potential, EV1, Engel–Vosko 93 GGA exchange term is combined with the LSDA correlation term in the WIEN2k code, see LAPW0 which generates potential. The LAPW0 calculates the total potential by summing Coulomb and exchange–correlation potentials using the total electron (spin) density. In the second potential, EV2, a combination

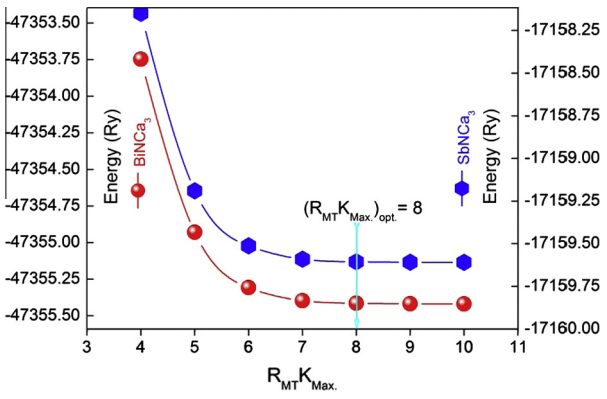

Fig. 1. Total energy of $BiNCa_3$ and $SbNCa_3$ compounds in Ry as a function of dimensionless $R_{MT}K_{Max.}$ parameter. The light down arrow indicates the optimized $R_{MT}K_{Max.}$ parameter, i.e., $(R_{MT}K_{Max.})_{Opt.}$.

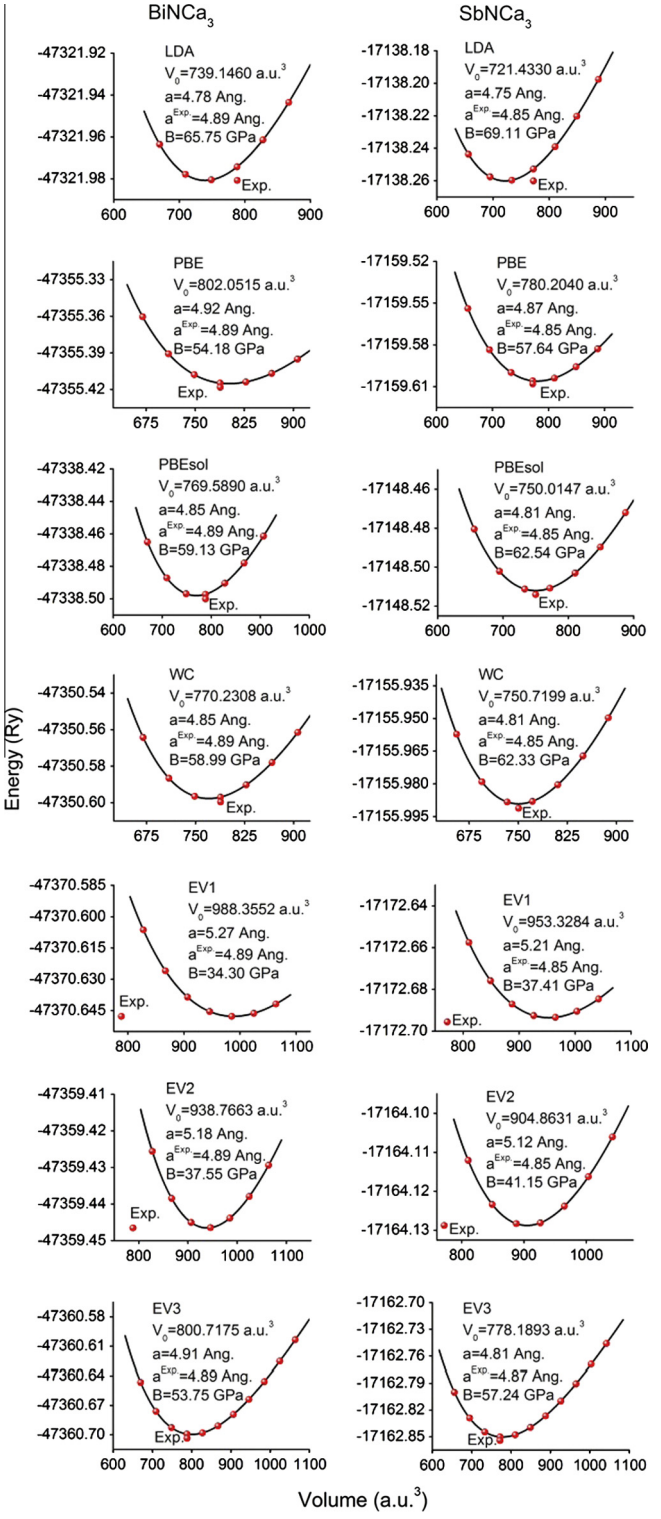

Fig. 2. Total energy in Ry as a function of volume in $Bohr^3$ fitted by Birch–Murnaghan equation of state within a variety of exchange–correlation functionals, i.e., LDA, PBE-GGA, PBEsol-GGA, WC, and three versions of Engel–Vosko-GGA. Experimental values are indicated for comparison. Left panel shows E–V curves of $BiNCa_3$, and right panel shows E–V curves of $SbNCa_3$.

of Engel–Vosko 93 GGA exchange term with Perdew–Wang 91 GGA correlation term is used in the LAPW0 of WIEN2k code. In the third EV3 potential option, Engel–Vosko 93 GGA exchange term, LSDA potential correlation term, Perdew–Wang 91 GGA exchange energy, and Perdew–Wang 91 GGA correlation term are

Table 1
Calculated equilibrium lattice constant *a* (Å) and bulk modulus B_0 (GPa) of $SbNCa_3$ and $BiNCa_3$compounds in comparison with experimental and other theoretical results.

Exchange–correlation	$SbNCa_3$	$BiNCa_3$
	Lattice constant a (Å)	
PBE-EV3	4.8674	4.9139
PBE-EV2	5.1183	5.1815
PBE-EV1	5.2081	5.2712
WC	4.8094	4.8507
PBEsol	4.8079	4.8494
PBE-GGA	4.8716	4.9166
LDA	4.7561	4.7846
Exp.	4.8541[a]	4.888[a]
Other theo.	4.732[b], 4.8 [c]	4.783[b], 4.85[c]
	Bulk modulus B_0 (GPa)	
PBE-EV3	57.2368	53.7518
PBE-EV2	41.1529	37.5455
PBE-EV1	37.4067	34.3033
WC	62.3284	58.9990
PBEsol	62.5424	59.1330
PBE-GGA	57.6427	54.1805
LDA	69.1133	65.7533
Other theo.	72.48[b], 55.42[b]	65.89[b], 54.01[b]

[a] Exp [7].
[b] GGA[11].
[c] Anylatical [18].

Table 2
Band gaps (in eV) for $SbNCa_3$ and $BiNCa_3$ by mBJ, EV-GGA, GGA and LDA.

Exchange-correlation	$SbNCa_3$	$BiNCa_3$
mBJ	1.1	1.09
GGA-EV3	0.84	0.80
GGA	0.42	0.40
LDA	0.40	0.38
Other theoretical		0.28[a], 0.07[b]

[a] LDA [9].
[b] LDA [8].

combined in the LAPW0 of the WIEN2k code. Results obtained from the different theoretical models are presented in Table 1. The calculated results are also compared with the experimentally measured values and other theoretical data. The table clearly indicates that our results are in good agreement with the other available data. The results show that the EV1 and EV2 cannot satisfactorily predict the lattice parameters. The table also reveals that PBE-GGA, and PBEsol, as well as EV3 are more appropriate techniques than the others for the calculations of the lattice parameters of these compounds, while EV1, EV2, and LDA may not be considered as suitable approximations if we compare the results with the experimental data. The shortcoming of the EV1 and EV2 is that they improve the properties that depend on the exchange potential, such as the electronic properties, but not those depend on the exchange–correlation energy. Therefore, EV1 and EV2 yield unsatisfactory results for properties that depend on the exchange–correlation energy such as structural properties and forces. From Table 1 and Fig. 2, it is clear that it is the GGA-PBE and EV3 which provide better values of the lattice constants than EV1 and EV2, compared to the measured results. No experimental data about the bulk moduli of these compounds is available in literature, to the best of our knowledge, for comparison. The lattice constant of $SbNCa_3$ is smaller than the lattice constant of $BiNCa_3$,

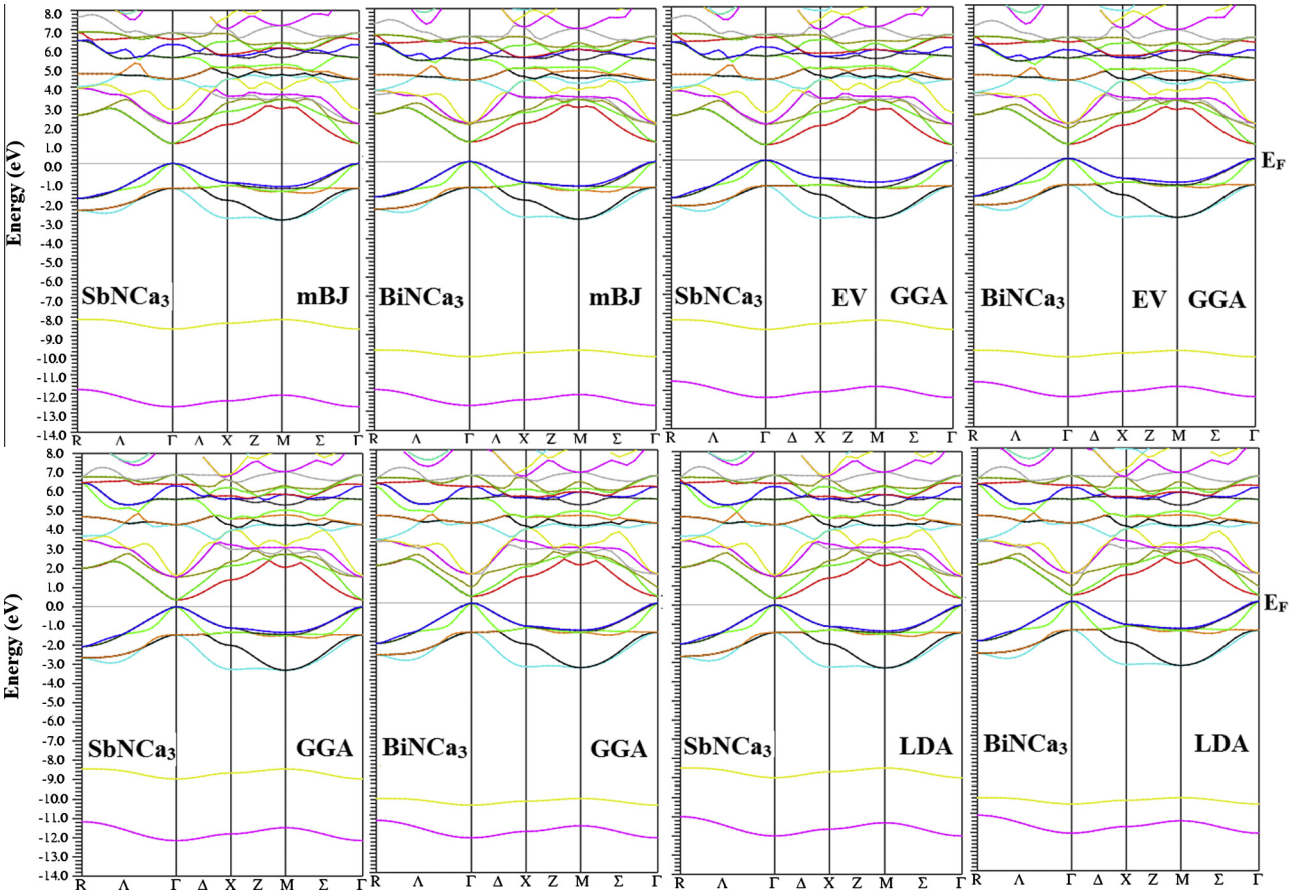

Fig. 3. Band structures for $SbNCa_3$ and $BiNCa_3$ by mBJ, EVGGA, GGA and LDA.

which is due to the fact that the radius of Sb (R_{Sb} = 1.4 Å) is smaller than the radius of Bi (R_{Bi} = 1.56 Å). It shows that the lattice constant increases with the increase in the atomic size of A atom. Unlikely, the bulk modulus decreases with the increase in the atomic size of the A site element which is in concurrence with the well-known relationship between B and lattice constant, i.e., $B\alpha V^{-1}$, where V is volume of the unit cell.

3.2. Electronic band structures and densities of states

The experimentally demonstrated semiconducting behavior of $SbNCa_3$ and $BiNCa_3$ compounds [7] has not been extensively investigated by any theoretical work, and therefore needs careful analysis to ensure the real picture of these compounds. In the present work, the electronic properties of these compounds in the cubic phase are investigated using four functionals, i.e., LDA, GGA, EV-GGA and mBJ. The calculated band structures by all the four models are illustrated in Fig. 3. The careful examination of the band profiles shows that for the same compound the band structures obtained by different models are similar with minor differences in details, whereas they are different for different compounds. The results obtained by all the four functionals depicted in the figures indicate that $SbNCa_3$ and $BiNCa_3$ are direct bandgap semiconductors, which is consistent with the experimentally observed nature of these compounds [7] and contradicts with the theoretical results [11]. The calculated band gaps for these materials are presented in Table 2. It is clear from the table that LDA provides the smallest, while mBJ gives the largest band gaps for these materials. Similar to LDA, GGA also underestimates [19,20] band gaps but it provides relatively better results. This is due to the fact that LDA assumes constant electron density for a system whereas in real the charge density is not uniform. However, GGA also has its limitations, as it does not reproduce both exchange–correlation energy and its charge derivative [21]. To overcome this problem, Engel and Vosko [22] designed a new functional form of the GGA at the expense of less agreement in exchange energy. As LDA and GGA are notorious for the underestimation of band gaps and mBJ is effective in the estimation of band gaps, hence in the present study we can rely on the mBJ potential and expect that the experimental band gaps for both of these compounds will be consistent with the results obtained by mBJ, i.e., 1.1 eV (Fig. 3 and Table 2). Despite using small number of k-points for mBJ as compared to the other three functionals, we get the largest band gap by mBJ, which shows mBJ is the best potential for studying the electronic structure for these materials. It is well understood that mBJ works well for the band gap calculations as compared to LDA and GGA, because of the extra exchange potential, not only for transition metal compounds but also for sp-type semiconductors [15].

The clear picture of the electronic properties of $SbNCa_3$ and $BiNCa_3$ compounds can be obtained from the total and partial density of states (DOS), depicted in Fig. 4. It is clear from the figure that both materials have approximately same DOS curves with a small difference in details. It can be seen from the figure that the region below the Fermi level is divided into two regions; semi-core and valance states. The semi-core states, lying between −11.5 eV and −12.8 eV for both materials, are entirely composed of nitrogen s states while semi-core states, lying between −8 eV to −8.7 eV for $SbNCa_3$ and −9.7 eV to −10.3 eV for $BiNCa_3$, are dominated by Sb/Bi-s states. In the upper valence band, states are mainly occupied by nitrogen p state, which is strongly hybridized with Sb/Bi-p states. The band gaps of 1.1 eV and 1.09 eV for $SbNCa_3$ and $BiNCa_3$ are also confirmed by the corresponding DOSs, respectively. The conduction band is dominated by Ca-d states with a mixture of Sb/Bi and N-p states showing hybridization. It is also worth noting that the amplitude of Bi-s states is higher in $BiNCa_3$ than the amplitude of Sb-s states in $SbNCa_3$ and the amplitude of N-p states is higher in $BiNCa_3$ than the amplitude of N-p states in $SbNCa_3$.

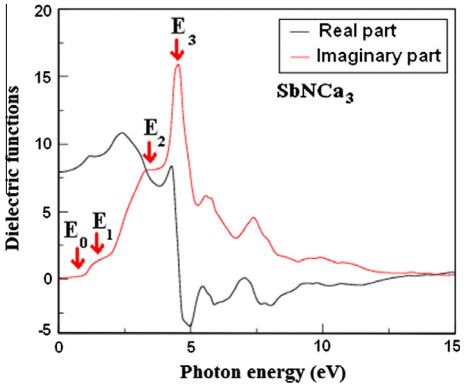

Fig. 5. Dielectric function $\varepsilon(\omega)$ for $SbNCa_3$ by mBJ.

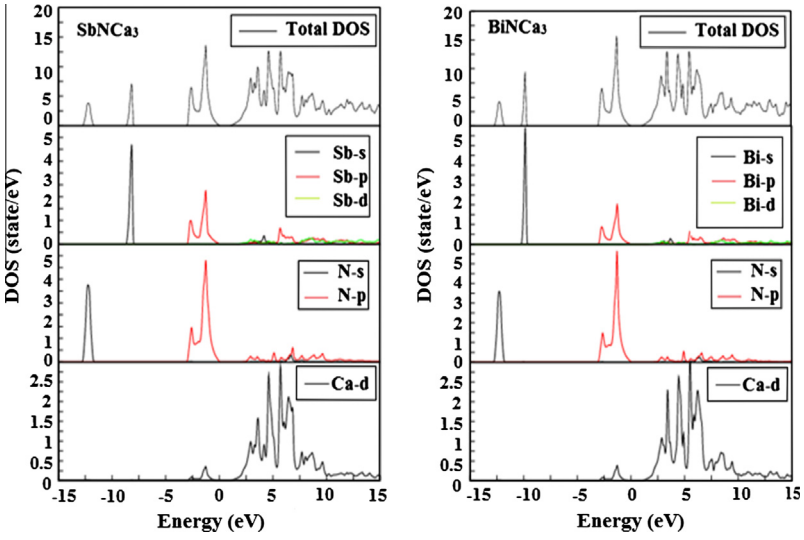

Fig. 4. Density of states (DOS) for $SbNCa_3$ and $BiNCa_3$ by mBJ.

3.3. Optical properties

Optical properties of a material are very helpful to identify the internal character of that material. The real and imaginary parts of the dielectric function, refractive index and absorption spectrum are calculated to observe the response of $SbNCa_3$ and $BiNCa_3$ to the applied electromagnetic field. The calculated optical properties for these materials with the mBJ formalism are presented in Figs. 5–8. It is clear from the figures that both materials show approximately same behavior with small differences in details.

The dielectric function $\varepsilon(\omega)$, consists of real part $\varepsilon_1(\omega)$ and an imaginary part $\varepsilon_2(\omega)$. The calculated results for $\varepsilon_1(\omega)$ and $\varepsilon_2(\omega)$ are presented in Figs. 5 and 6 for $SbNCa_3$ and $BiNCa_3$, respectively.

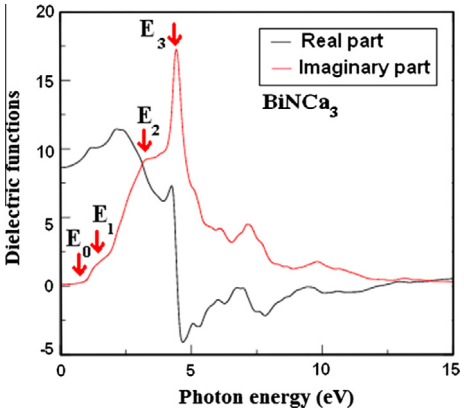

Fig. 6. Dielectric function $\varepsilon(\omega)$ for $BiNCa_3$ by mBJ.

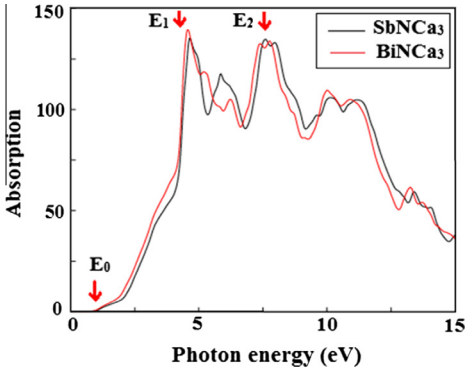

Fig. 7. Absorption coefficient for $SbNCa_3$ and $BiNCa_3$ by mBJ.

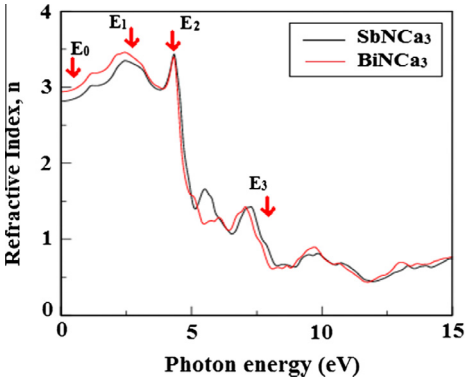

Fig. 8. Refractive index for $SbNCa_3$ and $BiNCa_3$ by mBJ.

The value of the static dielectric constant $\varepsilon_1(0)$ for $SbNCa_3$ is 7.8 and for $BiNCa_3$ is 8.5. The $\varepsilon_1(\omega)$ increases steadily with energy and reaches to its peak value at 2.36 eV for $SbNCa_3$ and 2.1 eV for $BiNCa_3$. Then it decreases to minimum negative value at 4.9 eV for $SbNCa_3$ and 4.6 eV for $BiNCa_3$. Collective excitations of large effective mass in the interfaces induced by electric field may be responsible [23] for the negative $\varepsilon_1(\omega)$ showing absorption in this energy range. After this point, it increases with some variations and becomes positive after 12.5 eV for both materials. The imaginary part $\varepsilon_2(\omega)$, presented in these figures clearly show the critical point (E_0) at 1 eV for these materials, which also confirms the band gap. After this point, we have a threshold (E_1) for transition from valance to conduction band. For higher energies, $\varepsilon_2(\omega)$ keeps increasing which shows steady increase in absorption up to 3.2 eV (E_2). In the energy range from 3.2 eV to 3.9 eV, the curve stays at the same point and shows constant absorption for $SbNCa_3$ but slowly increase for $BiNCa_3$. After this point, we see a sharp increase in the curves for both materials and receive peaks at 4.5 eV (E_3), where materials show maximum absorption. The absorption curves, in Fig. 7, also confirm this pattern as we see zero absorption up to 1 eV (E_0). At higher energies, we see peaks at 4.5 eV (E_1) and 7.5 eV (E_2), hence, the materials can be used as filters in this energy range of ultraviolet spectrum. Fig. 8 shows refractive index $n(\omega)$ for these materials. At zero energy the value of $n(\omega)$ is 2.8 (E_0) and 2.92 for $SbNCa_3$ and $BiNCa_3$ respectively. $n(\omega)$ reaches to maximum value at 4.3 eV (E_1) for $SbNCa_3$and 2.4 eV (E_2) for $BiNCa_3$.

4. Conclusions

In summary, we investigated the structural, electronic and optical properties of the antiperovskites $SbNCa_3$ and $BiNCa_3$ using the full potential linearized augmented plane waves method (FP-LAPW) within density functional theory. For the reliability of the work we used LDA, GGA and GGA-EV exchange correlation potentials. We found the lattice constants and bulk moduli are in good agreement with the available experimental data. For the batter band gaps, we also used mBJ, which gives the largest band gaps than all other potentials. All these potentials show that these materials are direct band gap semiconductors. LDA provides the smallest band gaps in comparison to the other potentials. The calculated band gaps using mBJ are 1.1 eV and 1.09 eV for $SbNCa_3$ and $BiNCa_3$ respectively which are expected to be the experimental band gaps of these compounds. The imaginary part of the dielectric function also confirms these band gaps for the materials.The materials show maximum absorption at 4.5 eV and then at 26 eV. Hence, in these energy ranges of ultraviolet spectrum the materials can be used as filters.

References

[1] W.S. Kim, E.O. Chi, J.C. Kim, H.S. Choi, N.H. Hur, Solid State Commun. 119 (2001) 507.
[2] E.O. Chi, W.S. Kim, N.H. Hur, Solid State Commun. 120 (2001) 307.
[3] A. Bouhemadou, R. Khenata, Comput. Mater. Sci. 39 (2007) 803.
[4] C.M.I. Okoye, Mater. Sci. Eng., B 130 (2006) 101.
[5] A.L. Ivanovskii, Russ. Chem. Rev. 64 (1995) 499.
[6] A.L. Ivanovski, R.F. Sabiryanov, A.N. Skazkin, Phys. Solid State 40 (1998) 1516.
[7] M.Y. Chern, D.A. Vennos, F.J. DiSalvo, Solid State Chem. 96 (1992) 415.
[8] D.A. Papaconstantopoulos, W.E. Pickett, Phys. Rev. B 45 (1992) 4008.
[9] P.R. Vansant, P.E. Van Camp, V.E. Van Doren, Phys. Rev. B 57 (1998) 7615.
[10] K. Haddadi, A. Bouhemadou, L. Louail, S. Maabed, D. Maouche, Phys. Lett. A 373 (2009) 1777.
[11] M. Moakafi, R. Khenata, A. Bouhemadou, F. Semari, Ali H. Reshak, M. Rabah, Comput. Mater. Sci. 46 (2009) 1051.
[12] O.K. Andersen, Phys. Rev. B 12 (1975) 3060.
[13] W. Kohn, L. Sham, Phys. Rev. 140 (1965) 1133.
[14] P. Blaha, K. Schwarz, G.K.H. Madsen, D. Kvasnicka, J. Luitz, Wien2k—An Augmented Plane Wave Plus Local Orbital Program for Calculating the Crystal Properties, Karlhein Schwarz, Vienna University of Technology, Austria, 2001.
[15] F. Tran, P. Blaha, Phys. Rev. Lett. 102 (2009) 226401.

[16] A.D. Becke, E.R. Johnson, J. Chem. Phys. 124 (2006) 221101.
[17] F.D. Murnaghan, Proc. Nat. Acad. Sci. USA 30 (1944) 244.
[18] B.V. Beznosikov, J. Struct. Chem. 44 (2003) 885.
[19] P. Dufek, P. Blaha, K. Schwarz, Phys. Rev. B 50 (1994) 7279.
[20] G.B. Bachelet, N.E. Christensen, Phys. Rev. B 31 (1995) 879.
[21] S. Labidi, H. Meradji, M. Labidi, S. Ghemid, S. Drablia, F. El Haj Hassan, Phys. Procedia 2 (2009) 1205.
[22] E. Engel, S.H. Vosko, Phys. Rev. B 47 (1993) 13164.
[23] C.W. Chu, F. Chen, J. Shulman, S. Tsui1, Y.Y. Xue, W. Wen, P. Sheng, SPIE Proc. 5932 (2005) 31.